SFH6, 2017-2018

AQA Extended Project Qualification

Lift Production - an optimal aerofoil design

Joe Binns, joebinns.95@gmail.com

Contents

Abstract

An aerofoil is a structure designed to give the greatest ratio of lift to drag. They are frequent in aviation, wind power and everyday appliances. I aim to establish coherent explanations for the mechanics of lift production and a thorough analysis of classic foil designs. With the use of Computer Aided Design and Computational Fluid Dynamics, I will produce optimal aerofoil shapes for various applications.

My early explanations regarding lift will be focused towards the functions of a fixed foil aircraft (such as an aeroplane). Once the foundations are established, we will begin exploring unfamiliar scenarios.

(Goossens, Airfoil, 2015)

Staying aloft, how to fly

Lift is the mechanical force that acts perpendicular to an oncoming flow. It typically acts opposite to the weight (with slight variations for controlling the motion of the aircraft).

We can interpret the effects of these forces on the motion of the body using Newton's second law of motion, which demonstrates that:

→If lift is greater than weight, the object will accelerate upwards.

→If lift is less than weight, the object will accelerate downwards.

→If lift is equal to weight, the object will remain at a steady velocity (or at rest).

Various processes take place which contribute to lift. The most significant processes are due to the conservation of momentum and conservation of energy in a fluid.

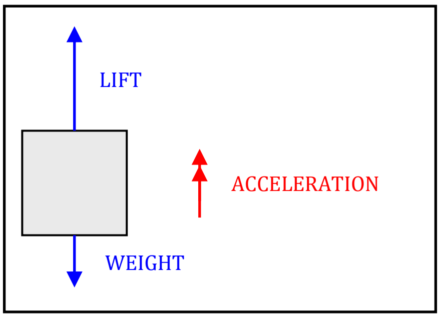

Fig 1, Newton's second law of motion

Conservation of energy in a fluid...

We will consider energy in a fluid to be comprised of *Fluid Pressure*, *Fluid Kinetic energy* and *Fluid Potential energy*. 'Fluid' is recurrent with aerodynamic variables; it simply means that the respective value will be given as a density (e.g. energy → energy density), meaning quantity per unit volume.

Fluid Pressure:

$$P = {}^{F}\!/_{A} = {}^{F \cdot d}\!/_{A \cdot d} = {}^{W}\!/_{V}$$

(P is pressure, F is force, A is area, d is distance, W is energy and V is volume)

The derivation above shows that pressure can be considered as energy per unit volume or '*energy density*'. The energy seen here, 'pressure energy', is a result of the thermal motions of atoms. It can therefore be considered as kinetic energy. It differs from Fluid Kinetic energy due to its random nature and should be considered individual. An easy way of separating them is to consider Fluid Pressure on the micro-scale and Fluid Kinetic energy on the macro-scale.

Fluid Kinetic energy:

$$ {}^{E_k}\!/_{V} = {}^{\frac{1}{2}mv^2}\!/_{V} = \tfrac{1}{2}\rho v^2$$

(E_k is kinetic energy, V is volume, m is mass, v is velocity and ρ is mass density)

Fluid Kinetic energy is the kinetic energy density of the fluid itself (as a flow, exclusive of thermal kinetic energies).

Fluid Potential energy:

$$ {}^{E_p}\!/_{V} = {}^{mgh}\!/_{V} = \rho g h$$

(E_p is potential energy, V is volume, m is mass, g is acceleration due to gravity, h is height and ρ is mass density)

Fluid Potential energy is the gravitational potential energy density of the fluid.

Daniel Bernoulli's equation:

$$Fluid\ Pressure + Fluid\ Kinetic\ energy + Fluid\ Potential\ energy = Total\ energy$$

$$ {}^{W}\!/_{V} \quad + \quad \frac{1}{2}\rho v^2 \quad + \quad \rho g h \quad = Total\ energy$$

Daniel Bernoulli applied a direct application of the conservation of energy to a fluid in motion, described by the Bernoulli equation.

Since the *Total energy* of a closed system is constant (by the conservation of energy), we can explore the effects of changing the variables above. If we are to assume change in *Fluid Potential energy* is negligible (due to a fairly constant mass density, acceleration due to gravity and height), then an increase in *Fluid Kinetic energy* will result in a decrease in *Fluid Pressure* (and vice versa).

$$Fluid\ Kinetic\ energy \propto {}^{1}/_{\sqrt{Fluid\ Pressure}}$$
$$Velocity \propto {}^{1}/_{\sqrt{Fluid\ Pressure}}$$

Limitations of the Bernoulli Equation:

By modelling fluids as multiple moving particles, we can see that the velocity will typically not be constant (either the direction or magnitude) in a fluid. We can therefore only give *Fluid Kinetic energy* as a function of the average velocity in the Bernoulli equation. *Turbulent flow* would involve motions in various directions (both the horizontal and vertical planes) and is therefore non-applicable. Therefore, the *Fluid Kinetic energy* must be acting in a single direction (a *laminar flow*), for this equation to be valid. Even in assuming a laminar flow, the velocity is not constant for all the particles and so we rely on average velocity.

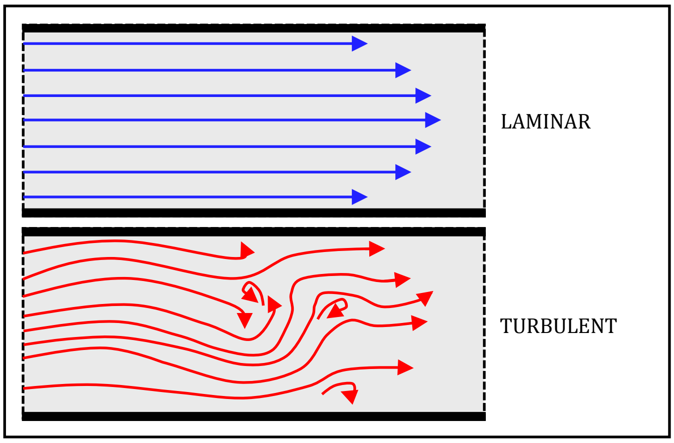

Fig 2, Laminar and Turbulent flow.

Bernoulli's equation is also limited by assuming no energy loss to the surroundings (e.g. conversion to thermal energy) and by not taking viscous drag effects into account.

Due to these limitations (as well as others), the Bernoulli Equation will only be referred to for its descriptive values.

Lift

Lift is generated when a fluid moving relative to a body is redirected towards weight. When a body is immersed in a fluid, the entire surface of the body is in contact with the fluid and thus the entire body contributes to the production of lift. The primary factors effecting lift are…
→ Geometry of the body; shape and size,
→ Motion; relative velocity and angle of attack*
→ and properties of the fluid; density, viscosity and compressibility.

A body immersed in a flowing fluid has two stagnation points, one at the front of the body and one at the rear (relative to the flow). The stagnation point is where the velocity of the fluid is zero; it can be considered the point of least velocity/greatest pressure in practicality. The front stagnation point is where the fluid will split in order to travel either above or below the body. In a similar fashion, the rear stagnation point is where the fluid will meet after splitting.

Viscosity is a measure of a fluids resistance to flow. The viscosity of a fluid causes flow and the surrounding flow to pursue the curve of a body, even after contact with the body. Due to this effect, the viscosity of a fluid can prevent fast-moving flows above and below the body from re-joining at the rear stagnation point. This is often the case with asymmetrical bodies and/or large angles of attack.

The positive angle of attack shown causes this symmetrical aerofoil to have a rear stagnation point on the upper side of the aerofoil. Due to the viscosity of the fluid and the great relative velocity, the fluid beneath the aerofoil cannot directly reach the rear stagnation and thus a vortex is created. This vortex remains stationary (downstream) whilst the aerofoil continues moving, eventually dispersing. The vortex shown has a counter-clockwise rotation. Due to the conservation of angular momentum, a vortex of the same magnitude acting in the opposite rotation must be present. This second clockwise vortex acts on the fluid flowing around the aerofoil. Since the vortex is in the same direction as the flow above the aerofoil, the flow has a greater velocity. Likewise, the vortex acts against the flow below the aerofoil, and so the flow beneath the aerofoil has a lesser velocity. By applying Bernoulli's equation, we can see that there will be a greater pressure beneath the aerofoil than there is above the aerofoil.

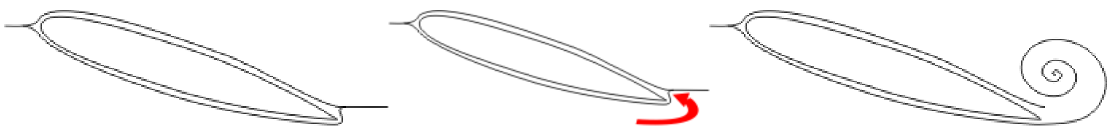

Fig 3, Formation of the initial vortex

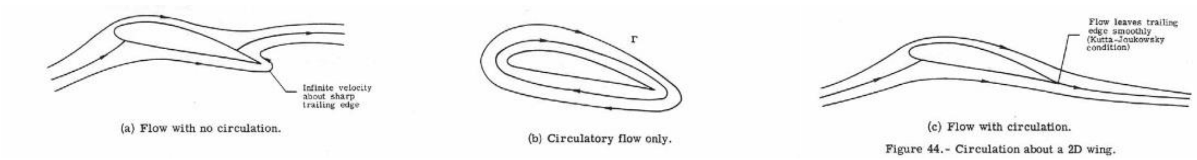

Fig 4, Formation of the secondary vortex

$$P = {}^{F}/_{A} = {}^{F \cdot d}/_{A \cdot d} \left(= {}^{W}/_{V}\right) \qquad \therefore P \propto F$$

Since Fluid Pressure is proportional to Force, there is a lesser force exerted on the top of the aerofoil and a greater force exerted on the bottom of the aerofoil. The result is a net upwards force acting on the aerofoil; this is lift on the aerofoil by the conservation of energy in a fluid.

---

* Angle of attack is the angle at which the chord of an aerofoil is inclined relative to the mean direction of oncoming flow.

Conservation of momentum…

Flow tends to pursue the curve of an aerofoil due to the Coandă effect.[†] This means that aerofoils with a downwards curve will redirect the oncoming flow downwards. By redirecting the flow of the fluid downwards, the fluid gains a downward velocity and thus gains a downward momentum.

$$p = m \cdot v$$

(p is momentum, m is mass and v is velocity)

$$momentum_{fluid} + momentum_{aerofoil} = Total\ momentum$$
$$p_{fluid} + p_{aerofoil} = Total\ momentum$$

Since *Total momentum* of a closed system is constant, the increase in the downwards momentum of the fluid causes the momentum of the aerofoil to increase in the opposite direction, upwards. Newton's second law of motion states that force is the rate of change of momentum. Therefore, the increased upwards momentum of the aerofoil can be given as an upwards force. This force is lift on the aerofoil by the conservation of momentum.

$$F = \Delta\langle {}^{p}/_{t} \rangle$$

(F is force, p is momentum and t is time)

(Hall, What is Lift?, 2015)

[†] The Coandă effect describes how a fluid tends to follow the curvature of a surface after losing contact with the surface.

Drag

Drag is generated when a fluid moving relative to a body resists the motion of the body. Many of the factors affecting drag also affect lift. Factors affecting drag are very much the same as those affecting lift. Changing the shape of an aerofoil will affect lift and drag in different ways. Within definite conditions (such as length), the shape of an aerofoil can be optimised for efficiency, so that the ratio of lift to drag is greatest. When approaching relative velocities near the speed of sound, shock waves form which produce an additional drag component.

Drag is caused by surface friction, the shape of the body and lift. The shape of the body redirects the fluid and is therefore responsible for a large amount of the drag force. By changing the shape of a body from a square to a sphere, drag is greatly reduced. Lift causes drag due to pressure differences above and beneath the aerofoil. The pressure difference causes a vortex to form at the tip of a three-dimensional aerofoil (similar to the vortex involved in lift, but at the tip of the aerofoil). The vortex flow produces a downstream force on the aerofoil, opposing the direction of motion and thus contributing to drag. Upwash caused by the tip vortex is theorised to be the reason for the V-shaped formation adopted by many species of birds during group flight.

Fig 5, Tip vortices in action

(Hall, What is Lift?, 2015)

Lift and drag relations

The lift to drag ratio is used to indicate the aerodynamic efficiency of an aerofoil. The greater the ratio, the better. At a constant velocity, greater lift allows for greater weights to be kept aloft, and minimising drag means a lesser thrust is required. Less thrust requires less energy and so mechanisms can run for more time at a lesser price.

Fig 6, Forces in flight

Since lift and drag are individually affected by the angle of attack, the ratio of lift to drag changes as the angle of attack changes. The figure below is for a given set of constant conditions (relative velocity, properties of air, etc.). The figure shows how we can determine the maximum ratio of lift to drag. You can see from the first graph that lift suddenly diminishes after an angle of attack of about 11 degrees. This is because the rear stagnation point raises so far up the upper surface that the effects of turbulence are so great that they outweigh the benefits of redirecting the flow further downwards. The maximum lift is obtained at the 'stall angle', where increasing the angle of attack any further will decrease the lift produced.

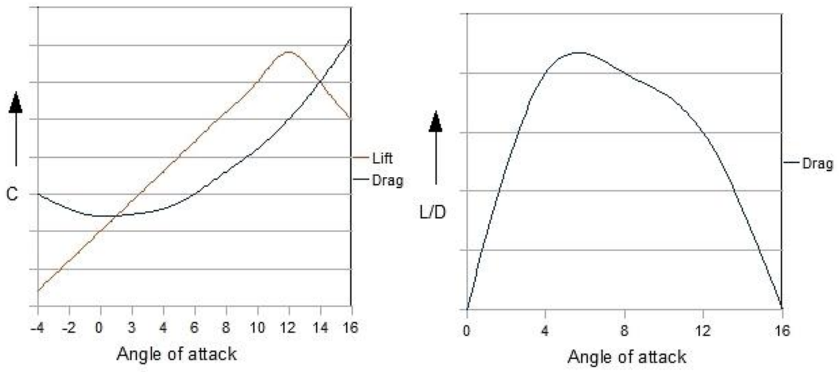

Fig 7, Graph of (the coefficients of) lift and drag against angle of attack
Fig 8, Graph of the ratio of lift to drag against angle of attack

The lift equation:

The lift equation approximates lift to be...

$$L = A \cdot C_L \cdot \left({}^{\rho \cdot v^2}/_{2} \right)$$

(L is lift, A is area, v is velocity, ρ is mass density and C_L is the lift coefficient‡)

... for a given object. Note that inside the parentheses is dynamic pressure.

We can use the lift equation to get a simplified idea of how lift is affected by various variables. We can see that

$$L \propto A,$$
$$L \propto v^2$$

‡ The lift coefficient is very complex and often determined experimentally for an object. The lift coefficient relies on multiple factors, such as the shape of the object and the viscosity of the fluid.

and $L \propto \rho$.

The drag equation:
In a similar fashion to the lift equation, the drag equation approximates drag to be...

$$D = A \cdot C_D \cdot \left({\rho \cdot v^2}/{2} \right)$$

... for a given object.

Therefore,

$$D \propto A,$$
$$D \propto v^2$$
and $D \propto \rho$.

(Goossens, Lift / Drag Ratio, 2015)
(Hall, Lift to Drag Ratio, 2015)

Ideal and non-ideal aerofoil shapes

Design criteria…

From ceiling fans to aircraft, the various applications of aerofoils have requirements which differ greatly. This is not even considering the different conditions in which an aerofoil might be applied; a reconnaissance aircraft landing on an aircraft carrier or at supersonic speeds in the stratosphere.

The different conditions and thus different variables (e.g. air property, relative velocity, etc.) require hugely different aerofoils for optimal performance.

Fig 9, Lockheed SR-71 Blackbird

Structural support…

By increasing some factors of an aerofoil shape to their extremes, the structural requirements of the aerofoil increase. For example, a thin aerofoil will be more prone to breaking than its thicker counterpart. In order to maintain the desired structural strength of the aerofoil, 'stronger' materials or supports will be required, potentially increasing the weight of the aerofoil. This counteracts the benefits of greater lift. We will therefore also consider the ratio of lift to weight in our models.

Camber and thickness…

Symmetrical aerofoils produce no lift at zero angle of attack whilst an asymmetrical aerofoil can produce significant lift. With angles of attack greater than zero, asymmetrical aerofoils are better able to redirect air downwards than their symmetrical counterpart. This allows asymmetrical aerofoils to produce greater lift prior to the stall angle. Therefore, asymmetrical aerofoils can have greater lift to drag ratios than symmetrical aerofoils.

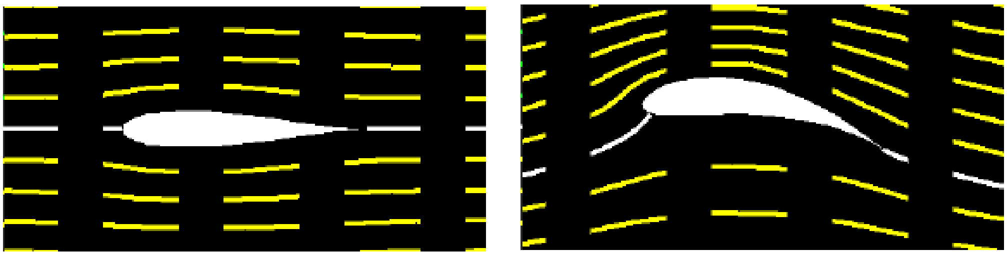

Fig 10, Effect of camber on an airflow

Excessive camber will result in the rear stagnation point raising so far up the upper surface so to create extreme turbulence, reducing lift. At greater velocities, the rear stagnation is more prone to change and so lesser cambers can be optimal. Thus there is a limit imposed on the camber of an aerofoil.

The thickness of an object is proportional to the weight of an object, so thinner aerofoils seem ideal. In action, an aerofoil must be thick enough to maintain its shape (to an extent) and not break under the aerodynamic stress. A typical middle ground considered to be optimal is a ratio of maximum thickness to chord length of about 12%, although this varies by a few percent depending on the application. For example, the ratio for a typical helicopter blade is about 15%.

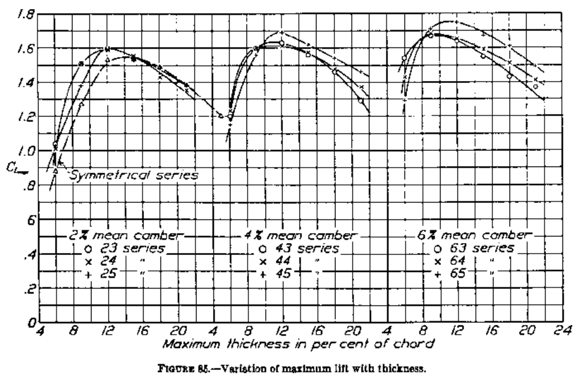

Fig 11, (Coefficient of) Lift against percentage thickness for increasing cambers

Aerofoil span…

From the relationship $L \propto A$, we can see that a greater area provides the potential for greater lift production. By increasing the aerofoil span, the area of the aerofoil increases by the same factor. Therefore, an aerofoil with a greater span will produce more lift in an approximately proportional relationship. However, the relationship $D \propto A$ also exists and so we must consider the lift to drag ratio and the application when determining the optimal span for an aerofoil. An aerofoil with a greater span also benefits from a diminished vortex at its tip (as described in the Drag section).

As the aerofoil span increases, the aerodynamic forces will increase and so the aerofoil will need to withstand greater stress. This has been historically problematic, leading to the infamous design of the red baron's three-winged plane. Multiple wings allowed for shorter wingspans and thus sturdier aerofoils. This is less common in modern designs due to material advancements providing materials able to withstand the greater stress experienced on longer wings.

Fig 12, Red Baron's Fokker Dr.1

Planform twist and taper…

An aerofoil with twist is one which has a changing angle of attack along its span. Twist manipulates the distribution of lift of an aerofoil. Twist is made effective in promoting a gradual stall from the root of the aerofoil to the tip rather than a more sudden stall which would occur otherwise. This benefits pilots by allowing them to better avoid unanticipated stalling and maintain rotary control of the aircraft prior to complete stall (since the ailerons[§] providing rotary control, located near the tips, will experience stall last).

The aerofoils of rotary-aerofoil aircraft typically do not have ailerons, and so a twist only benefits the aircraft with a more gradual stall. However, since the relative velocity increases from the root of the aerofoil to its tip[**], the optimal angle of attack will decrease down the span. Twist allows for optimal lift to drag ratios for a particular angular velocity.

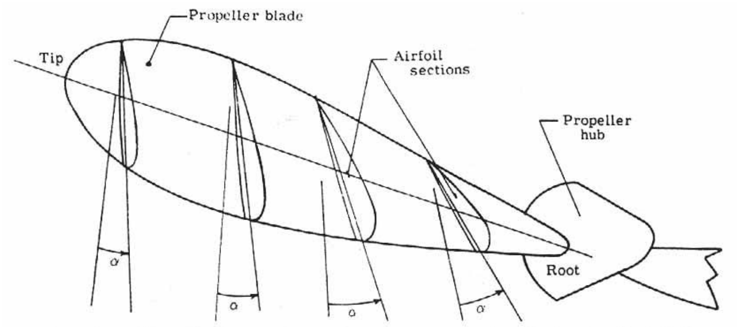

Fig 13, Example of twist and taper

Taper is when the chord length and/or thickness of an aerofoil reduces along its span. This causes the size and potentially the shape to change at different sections along the aerofoil. Tapering an aerofoil manipulates the distribution of lift. This is useful for minimising the vortices produced at the tips of an aerofoil by changing the size and shape tending towards the tip. For rotary-aerofoil aircraft, taper can be used to improve the lift distribution along the span of an aerofoil to one which is more consistent.

The Spitfire is one of few planes to exhibit a wholly elliptical planform. An elliptical planform is the most efficient, providing an optimal ratio of lift to drag for velocities less than the speed of sound ($< mach\ 1$). Few aircraft, such as the F-111A, have dynamic planforms which are able to appropriately transform for a given velocity (be it less than or greater than the speed of sound).

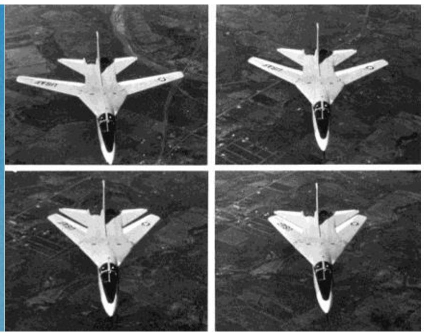

Fig 14, Supermarine Spitfire
Fig 15, General Dynamics F-111 Aardvark

(Goossens, Rotor Blade Design, 2015)
(Bethwaite, 2017)
(Hall, Shape Effects on Lift, 2015)
(Hall, Introduction to the Aerodynamics of Flight, 2015)
(Tangler)

§ Ailerons are the flaps located towards the wing tips of fixed-wing aircraft.
** Due to circular motion, $v = \omega \cdot r$ thus $v \propto r$.

Computational Fluid Dynamics

Computational Fluid Dynamics (CFD) computes the flow of a fluid through a given space and its forces of interaction with objects within the space. Recent developments in CFD and computation is making it a viable alternative to wind tunnel testing. I aim to make best use of the technology in order to provide consistent, meaningful results which will then undergo further analysis. I will base my models on the original National Advisory Committee for Aeronautics (NACA) aerofoil series, developed throughout the 1930s and revised in 1974. Although these older models are by no means optimal, the NACAs series is extremely coherent, allowing for diverse results and my own refinements.

The National Advisory Committee for Aeronautics' Five-Digit series:

The NACAs five-digit series describes the shape of an aerofoil.

The five-digit name of each aerofoil describes its shape. Each digit represents a characteristic of the aerofoil, such that:

$Digit\ one \rightarrow Maximum\ lift\ coefficient\ (at\ stall\ angle)\ divided\ by\ 0.15.$
$Digit\ two \rightarrow Product\ of\ percentage\ chord\ length\ to\ maximum\ camber\ and\ 5.$
$Digit\ three \rightarrow Simple\ (0)\ or\ reflex\ (1)\ curvature.$
$Digits\ four\ and\ five \rightarrow Percentage\ ratio\ of\ maximum\ thickness\ to\ total\ chord\ length.$

The airflow about the aerofoil and a graph of the ratio of the lift coefficient to the drag coefficient against the angle of attack will be analysed for each aerofoil in order to compare them, determine their theoretical optimal use and inspire the span form for my optimal aerofoil designs.

The conservation of momentum, energy and mass in the air flow must be considered for a fully developed understanding of the processes taking place. The conservation of momentum is described by Newton's laws of motions and the conservation of energy is described by the Bernoulli equation. Leonard Euler introduced the conservation of mass in a fluid to the conservation of momentum and energy described by Newton and Bernoulli. This is described by the Euler equations. The Navier-Stokes equations are a developed form of the Euler equations, taking viscosity into account. The Navier-Stokes equations are the common basis for CFD software.

I will be using Autodesk CFD to test the aerofoils, which are to be built and refined using Computer Aided Design (CAD) through Autodesk Fusion 360 and Autodesk Inventor.

CFD Results

A typical maximum cruise velocity for lightweight single engine aircraft such as the Cessna 172 is about 80 metres per second. I will be using this value, a chord length of 1 metre and a typical pressure of 1 atmosphere in my initial CFD testing and for estimating appropriate Reynolds numbers[††]. An appropriate range of Reynolds numbers have been selected. However, the maximum value available from the source is one million, whereas our conditions expect a Reynolds number of about five million.

Note that the Reynolds number is directly proportional to the chord length and the fluid velocity,

$$Re \propto l,$$
$$Re \propto v.$$

(Re is Reynolds number, l is chord length and v is velocity)

Fig 16, Graphs of the ratio of (the coefficients of) lift to drag, against angle of attack

[††] The Reynolds number is the general ratio of inertial forces to viscous forces for a particular fluid with given conditions. It is used to determine the way in which a fluid will flow, it is thus necessary for determining the coefficients of lift and drag.

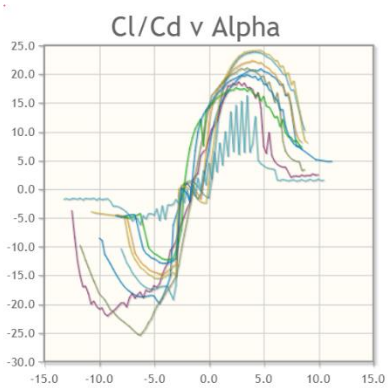

a) Re = 50,000

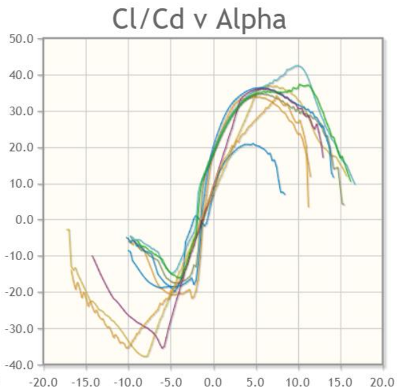

b) Re = 100,000

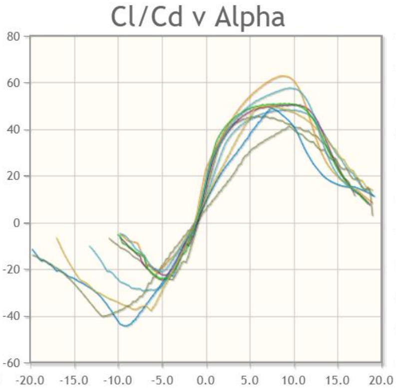

c) Re = 200,000

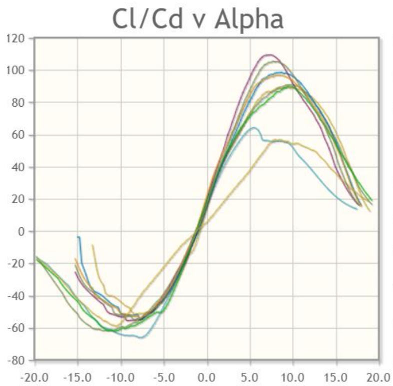

d) Re = 500,000

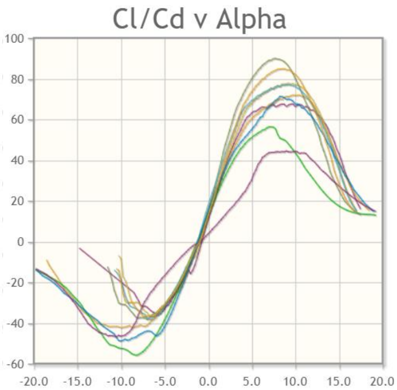

e) Re = 1,000,000

I will be extrapolating the maximum Cl/Cd and angle of attack values for a Reynolds number of 5,000,000 for all of the aerofoils, given the ratio of differences on the maximum Cl/Cd and angle of attack between previous Reynolds number increases of factor 5. Given that there are two sets of values for this factor increase, I will be able to numerically determine whether or not the ratio of differences is constant. This could be useful for determining the potential error of my extrapolated results.

Known values:

Reynolds Number	NACA identifier	α (°)	Max Cl/Cd
50,000	25112	2.5	17.7
	23021	2.75	18.6
	23024	3.5	16.3
	24112	3.5	19.9
	23018	3.5	21.1
	23112	4	22.3
	22112	4.25	23.9
	23015	4.75	21
	23012	4.75	24.2
100,000	25112	10	42.5
	23021	6.75	37
	23024	7.5	34.2
	24112	10.3	37.3
	23018	5.75	36.1
	23112	5.75	34.7
	22112	5	33.9
	23015	6.75	33.7
	23012	5.5	36.4
200,000	25112	8.75	62.9
	23021	7.5	49.1
	23024	9.5	41.3
	24112	9.5	57.7
	23018	7.25	50
	23112	10.3	50.6
	22112	6	45.7
	23015	9.5	48.4
	23012	9	51
500,000	25112	7.75	89.9
	23021	7.25	56.4
	23024	9	44.5
	24112	8.75	84.9
	23018	8.25	71.3
	23112	9.25	77.9
	22112	9.75	67.7
	23015	10.5	72
	23012	9	77.1
1,000,000	25112	7.5	109.4
	23021	5.5	64.3
	23024	8.5	56.9
	24112	7.75	105.5
	23018	9.5	89.9
	23112	8.75	98.6
	22112	9.25	89.4
	23015	10	91
	23012	8.75	96.8

Extrapolated values:

NACA identifier	ratio 1	ratio 2	mean ratio	Max Cl/Cd	Max Cl/Cd (2.d.p)
25112	1.73926868	2.115294118	1.927281399	210.8445851	210.84
23021	1.309572301	1.524324324	1.416948313	91.10977652	91.11
23024	1.377723971	1.301169591	1.339446781	76.21452183	76.21
24112	1.828422877	2.27613941	2.052281144	216.5156606	216.52
23018	1.798	1.975069252	1.886534626	169.5994629	169.60
23112	1.948616601	2.244956772	2.096786687	206.7431673	206.74
22112	1.956236324	1.997050147	1.976643236	176.7119053	176.71
23015	1.880165289	2.136498516	2.008331903	182.7582032	182.76
23012	1.898039216	2.118131868	2.008085542	194.3826805	194.38

NACA identifier	ratio 1	ratio 2	mean ratio	α	α (2.d.p)
25112	0.857142857	0.775	0.816071429	6.120535714	6.12
23021	0.733333333	1.074074074	0.903703704	4.97037037	4.97
23024	0.894736842	1.2	1.047368421	8.902631579	8.90
24112	0.815789474	0.853658537	0.834724005	6.46911104	6.47
23018	1.310344828	1.434782609	1.372563718	13.03935532	13.04
23112	0.853658537	1.608695652	1.231177094	10.77279958	10.77
22112	1.541666667	1.95	1.745833333	16.14895833	16.15
23015	1.052631579	1.555555556	1.304093567	13.04093567	13.04
23012	0.972222222	1.636363636	1.304292929	11.41256313	11.41

Reynolds Number	NACA identifier	α (°)	Max Cl/Cd
5,000,000	25112	6.12	210.84
	23021	4.97	91.11
	23024	8.90	76.21
	24112	6.47	216.52
	23018	13.04	169.60
	23112	10.77	206.74
	22112	16.15	176.71
	23015	13.04	182.76
	23012	11.41	194.38

Note that the set of ratios 1 and 2 are typically consistent with one another for each aerofoil's maximum ratio of coefficients values, suggesting that the extrapolated data should be accurate to an appropriate degree. However, this is not so much the case for the angle of attacks sets of ratios; the extrapolated angle of attack will therefore be a less accurate approximations.

Each Reynolds numbers aerofoil with the maximum ratio of coefficients has a green-shaded row. I discovered three different aerofoils which performed best over the range of Reynolds numbers, all of which were similar in shape.

NACA 24112:

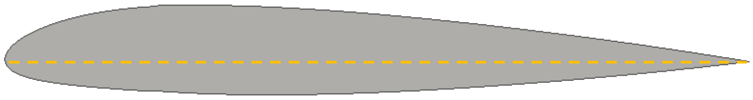

Fig 17, NACA 24112

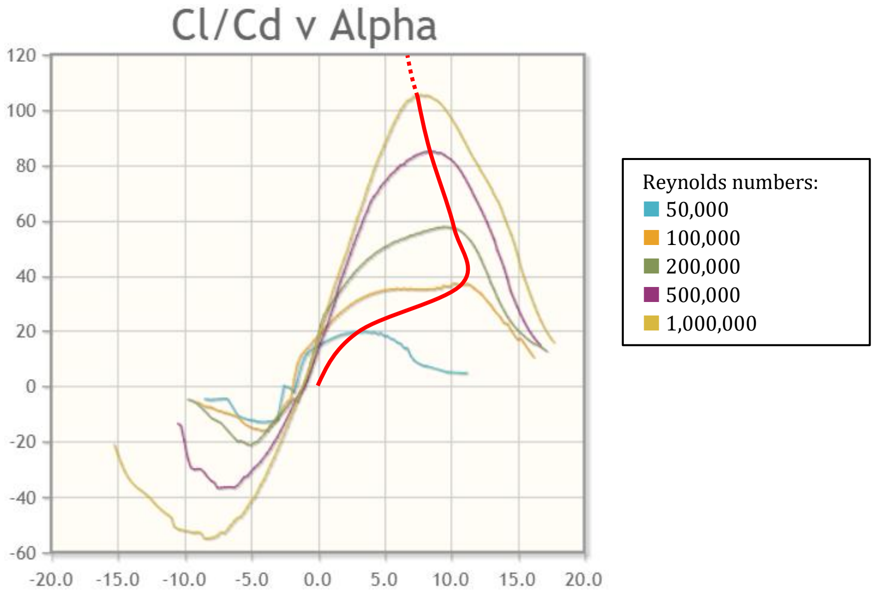

Fig 18, Graphs of the ratio of (the coefficients of) lift to drag against angle of attack (NACA 24112)

The solid and the dashed red line I have added shows the respective interpolated and extrapolated trend of the maximum ratio of coefficients against angle of attack.

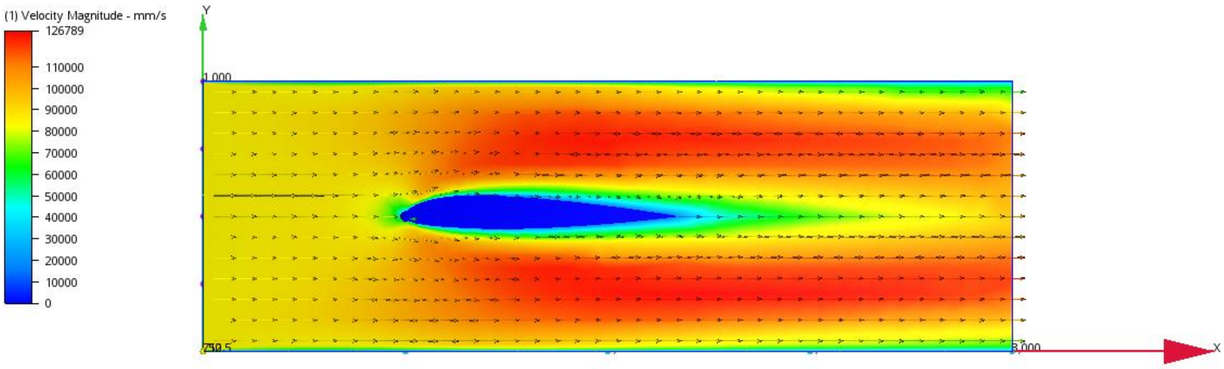

Fig 19, CFD solution at zero angle of attack (NACA 24112)

The CFD solution for this aerofoil displays the velocity magnitude of the fluid. Since there is a zero angle of attack, the magnitude of velocity above and below the aerofoil is near indistinguishable. Aerofoils can be visually compared using these graphs to assist in getting a general notion for the efficiency of a design. For example, the aerofoil below, which has a substantially lesser ratio of coefficients at this Reynolds number, is seen to have a significantly lesser fluid velocity prior to and after the aerofoil, suggestive of significantly increased drag as expected.

NACA 23021:

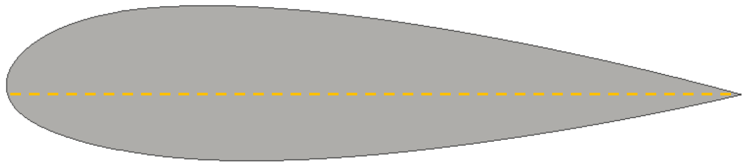

Fig 20, NACA 23021

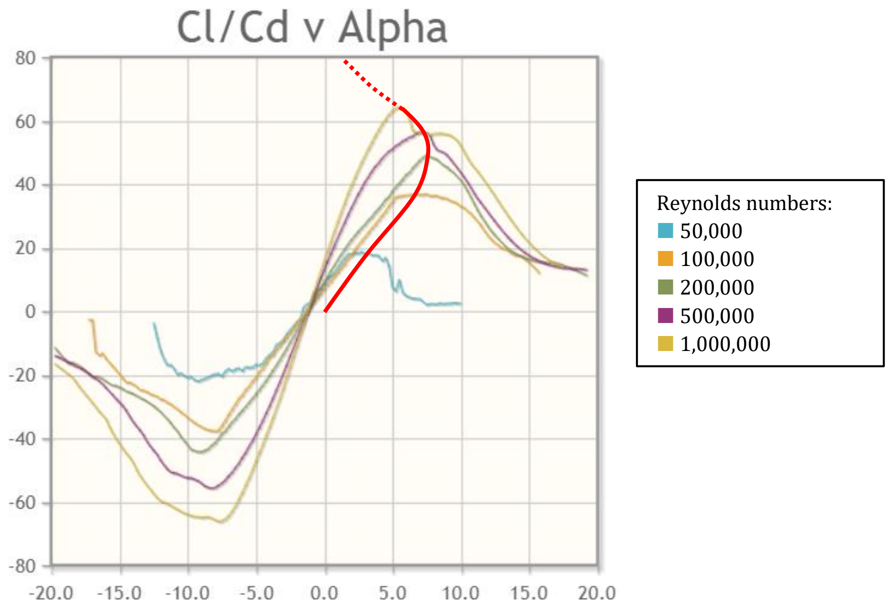

Fig 21, Graphs of the ratio of (the coefficients of) lift to drag against angle of attack (NACA 23021)

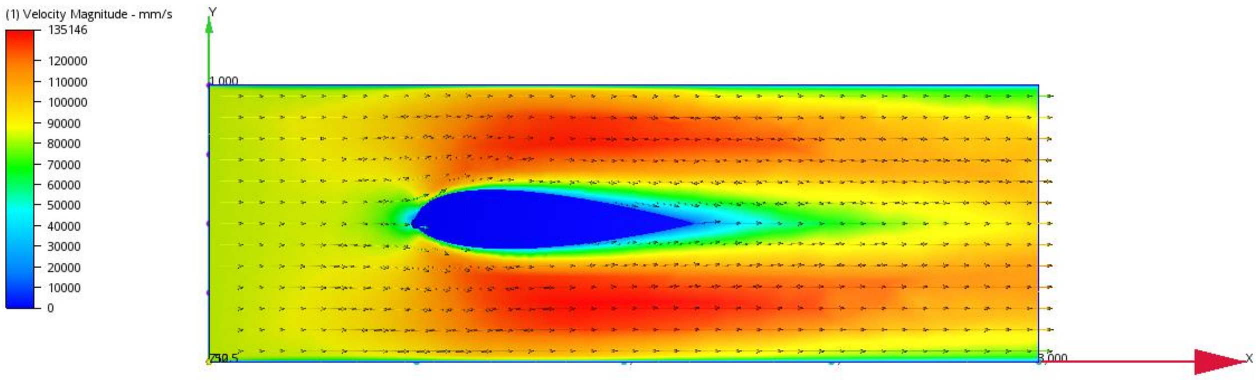

Fig 22, CFD solution at zero angle of attack (NACA 23021)

(Hall, Bernoulli and Newton, 2015)
(NACA 5 digit airfoil generator, 2017)

Aerofoil production

I have modelled my planform as an elliptical wing, a similar shape to that adopted by the Spitfire (chosen for reasons given earlier in 'Planform twist and taper'). I have decided to model the wing from four aerofoils, optimising the ratio of coefficients as the Reynolds number is reduced through greater taper (through the Reynolds number relationship with chord length). Each of the four aerofoils will be positioned at their optimal angle of attack for the respective Reynolds number.

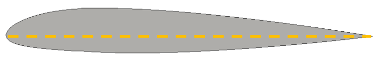

Fig 23, NACA 24112

Fig 24, NACA 25112

Fig 25, NACA 23012

The four aerofoils will be for chord lengths of 1m, 0.2m, 0.1m and 0.01m. These chord lengths have respective Reynolds numbers of five million, one million, five-hundred thousand and fifty thousand. The aerofoils used will be those previously identified as having the greatest ratio of coefficients for the respective Reynolds number. The result is illustrated below, showing the dimensions of the wing, along with the chosen aerofoils and their angles of attack.

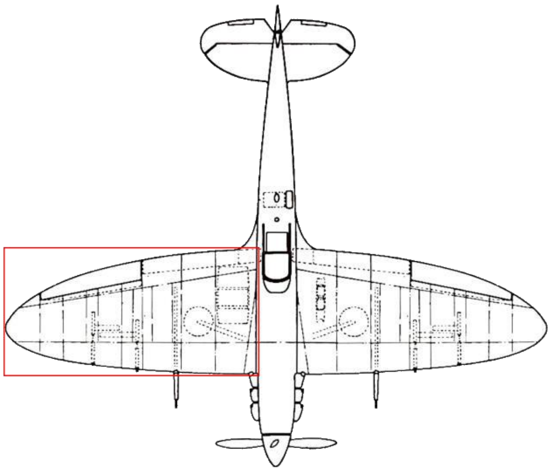

Fig 26, Supermarine Spitfire wing profile

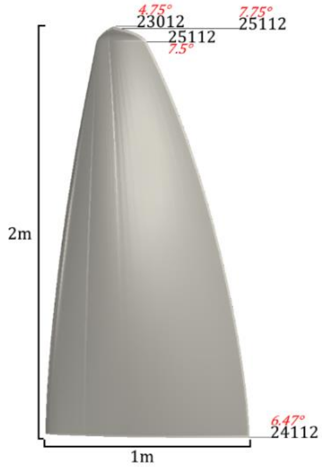

Fig 27, Wing design through CAD

The resultant wing has undergone CFD testing in order to experimentally determine whether or not it is exhibiting the expected behaviours of an optimal wing, as theorised. The images below illustrate the surface pressure of the fluid. There is a significantly greater pressure on the bottom of the aerofoil than the top of the aerofoil, as expected from a well-functioning wing.

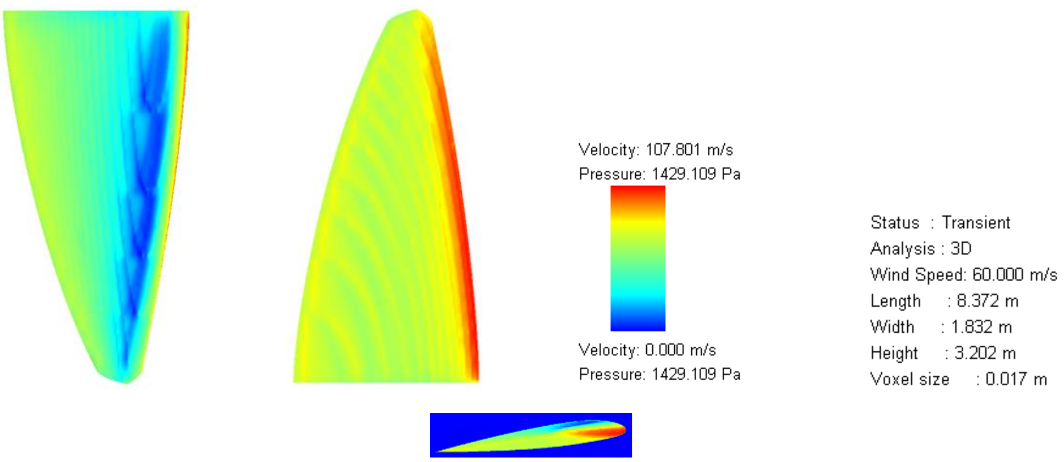

Fig 28, Wing surface pressure simulation through CFD

Reflections on the design

I believe that this approach to wing design could be the key to producing wings with optimal efficiency for use in certain, constant conditions. However, I do believe that generating a truly optimal aerofoil for given conditions would require an iterative approach, both in designing and choosing the aerofoils, and producing the wing itself. This would allow for various designs to be tested against one another and selected appropriately; a machine learning neuro evolution could potentially work well here.

The approach would also gain from more than four aerofoils at intervals of lesser Reynolds numbers for better results.

(Stanley, 2002)

Applications to fluid turbine designs

A 100% efficiency would cause fluid leaving the turbine to have no kinetic energy, preventing the flow of fluid. A 0% efficiency would allow unchanged flow of fluid but no kinetic energy would be harvested. Betz' law states the theoretical limit for which the kinetic energy of a fluid can be harvested as 59% of the total kinetic energy. This introduces a limit to the potential power efficiency of turbines. In reality, fluid leaving the turbine has rotary energy due to the tip vortices described earlier. This rotary energy gained by the fluid is useless and takes away from energy that would otherwise be made useful. At greater rotary velocities, their tip vortices are lesser and thus the turbine is more efficient. Turbines are therefore best fit for fast moving aerofoils, such as the classic three-bladed wind turbine design, rather than designs with more aerofoils that are slower moving (amongst other reasons such as cost efficiency).

Fig 29, Air turbine designs

(Proof of Betz' Law, 2003)

Bibliography

Bethwaite, F. (2017). *Design Tips*. Retrieved from Fast Composites: http://www.fastcomposites.ca/site/marine/design-tips-fabrication-overview/design-tips/

Goossens, P. (2015). *Airfoil*. Retrieved from Heli Start: http://www.helistart.com/Airfoil.aspx

Goossens, P. (2015). *Lift / Drag Ratio*. Retrieved from Heli Start: http://www.helistart.com/liftdragratio.aspx

Goossens, P. (2015). *Rotor Blade Design*. Retrieved from Heli Start: http://www.helistart.com/RotorBladeDesign.aspx

Hall, N. (2015, May). *Bernoulli and Newton*. Retrieved from NASA: https://www.grc.nasa.gov/WWW/K-12/airplane/bernnew.html

Hall, N. (2015, May). *Introduction to the Aerodynamics of Flight*. Retrieved from NASA: https://history.nasa.gov/SP-367/chapt4.htm#f42

Hall, N. (2015, May). *Lift to Drag Ratio*. Retrieved from NASA: https://www.grc.nasa.gov/www/k-12/airplane/ldrat.html

Hall, N. (2015, May). *Shape Effects on Lift*. Retrieved from NASA: https://www.grc.nasa.gov/www/k-12/airplane/shape.html

Hall, N. (2015, May). *What is Lift?* Retrieved from NASA: https://www.grc.nasa.gov/WWW/K-12/airplane/lift1.html

NACA 5 digit airfoil generator. (2017). Retrieved from Airfoil Tools: http://airfoiltools.com/airfoil/naca5digit

Proof of Betz' Law. (2003). Retrieved from Danish Wind Industry Association: http://xn--drmstrre-64ad.dk/wp-content/wind/miller/windpower%20web/en/stat/betzpro.htm

Stanley, K. O. (2002). Evolving Neural Networks through Augmenting Topologies. The MIT Press Journals. Retrieved from http://nn.cs.utexas.edu/downloads/papers/stanley.ec02.pdf

Tangler, J. L. (n.d.). The Evolution of Rotor and Blade Design . Retrieved from http://wind-works.org/cms/fileadmin/user_upload/Files/Jim_Tangler_VAWTs_AWEA2000b.pdf